1-1-2017

# Engineering A Retinal Progenitor Cell Graft For Transplantation Studies In The Rd10 Mouse Model

Maryam Ghiassi
*Yale University*

## Recommended Citation

Ghiassi, Maryam, "Engineering A Retinal Progenitor Cell Graft For Transplantation Studies In The Rd10 Mouse Model" (2017). *Yale Medicine Thesis Digital Library*. 2125.
https://elischolar.library.yale.edu/ymtdl/2125

**Engineering a Retinal Progenitor Cell Graft for transplantation studies in the RD10 Mouse**

**Model**

A Thesis Submitted to the

Yale University School of Medicine

in Partial Fulfillment of the Requirements for the

Degree of Doctor of Medicine and Master of Health Sciences

By

Maryam Ghiassi

2017

Abstract

In later stages of retinal degenerative diseases such as age-related macular degeneration (AMD) and retinitis pigmentosa stem cell therapy can be the only viable treatment option due to the loss of photoreceptor and RPE cells. Differentiation of embryonic stem cells (ESCs) towards the desired lineage explicitly requires a microenvironment that mimics the natural tissue that it is intended to regenerate. Developing a planar 3D retinal graft derived from ESCs can be transplanted to treat various retinal degeneration diseases. Our aim was to explore the differentiation and growth of ESCs on a gelatinous scaffold in order to transplant into a retinitis pigmentosa mouse model (RD10). Our aim was to evaluate the transplanted graft for host inflammatory response, stem cell integration, cell survival, and tumorigenesis. The transplanted graft was also compared to injection of a homogenous photoreceptor cell population into the subretinal space of the RD10 mouse model. A biocompatible gelatinous scaffold was developed in order to support the differentiation of a multilayered retinal structure. ESCs were seeded onto the scaffold for proliferation and differentiation in the vicinity of retinal pigment epithelium cells. Cultures were analyzed for differentiation by qRT-PCR and immunofluorescence confocal microscopy. The graft was transplanted into the subretinal space to examine biocompatibility and retinal progenitor cell integration into the native mouse retina. ESCs migrated through the $60\mu m$ thickness of the scaffold and differentiated into the retinal progenitor cells as evidenced by qRT-PCR and immunohistochesmistry. In-vivo testing analyzed on $1^{st}$, $3^{rd}$ and $6^{th}$ week showed scaffold degradation by the $6^{th}$ week. The gelatinous scaffold supported the differentiation of ESCs to RPCs and minimal inflammatory response was seen post transplantation.

Acknowledgements

I would like to thank Dr. Lawrence Rizzolo and Dr. Ron Adelman for their wonderful support and enthusiasm over the course of my year in the laboratory. They have been inspiring mentors, challenging me to take ownership of my project and develop my skills as a scientist and as a clinician. I want to also thank the senior members of the laboratory, Dr. Singh and Dr. Wang for their support and guidance as they taught me new skills and tremendously helped me along the way. I would also like to thank Laurel Tainsh for being a supportive and great lab-mate. I would Also like to thank my committee members, Dr. Chen and Dr. Niklason for their guidance and constructive comments throughout the year.

I thank Jason Thomson and Yinghong Ma at the Yale Stem Cell Core for their expertise, patience, and insightful discussions. I would also like to thank Dr. John Forrest, Donna Carranzo, and Mae Geter at the Office of Student Research for their support. I have had a tremendous experience in the past year and it was made possible through the one-year Gershon research fellowship grant.

I would lastly like to thank my wonderful family and friends for their support throughout my life. I would not have reached all these milestones without their encouragement, unconditional love and presence.

Table of Contents

**Introduction**

Retinal Degeneration and future Intervention Methods

Patients with retinal degenerative diseases have many pathways which are negatively affected in photoreceptor cells. Pathways such as phototransduction, lipid metabolism, RNA splicing, inner and outer segment formation of photoreceptor cells, vesicle trafficking and protein folding can be malfunctioning (1). The retinal pigment epithelium (RPE) underlying the photoreceptor layer, responsible for nourishing the retina, can have mutations in phagocytosis, light sensitive rhodopsin regeneration, and ion trafficking causing photoreceptor dysfunction and ultimately death of these cells (2,3).
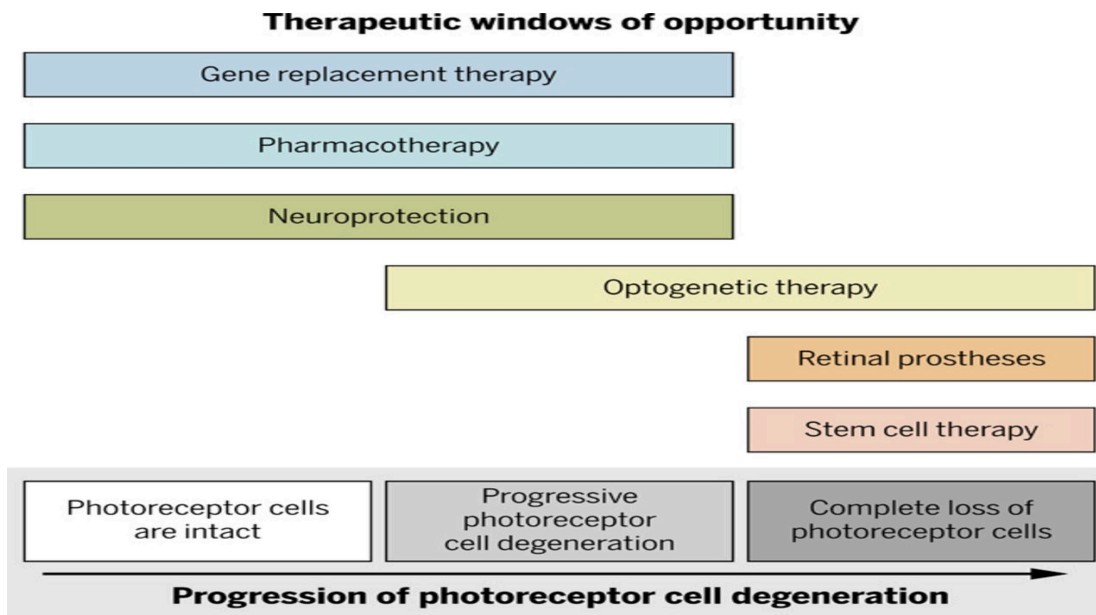
**Therapeutic windows of opportunity**

Gene replacement therapy

Pharmacotherapy

Neuroprotection

Optogenetic therapy

Retinal prostheses

Stem cell therapy

| Photoreceptor cells are intact | Progressive photoreceptor cell degeneration | Complete loss of photoreceptor cells |

**Progression of photoreceptor cell degeneration**

**Figure 1**- Strategies used to treat retinal degeneration at different time points. Gene therapy is used at earlier stages when the photoreceptors are intact. Pharmacotherapy and neuroprotective strategies are suitable in ongoing photoreceptor cell degeneration. Stem cell therapy, optogenetic therapy, and retinal prostheses are needed to restore vision during the later stages of retinal degeneration. (Figure adapted from 3a)

Pharmacotherapy or neuroprotective agents can be used in early stages of the disease when the photoreceptors are still viable. Gene therapy can be used when there is a single genetic mutation

that can be corrected using the CRISPR/Cas9 system or AAV vector transfection containing the corrected gene insert (4,5). However, in a heterogeneous retinal degenerative disease when there is not a single genetic mutation and in later stages of the disease when the photoreceptor cells are not viable, retinal stem cell replacement can be the only solution to vision restoration or preservation.

Retinal degenerative diseases such as age-related macular degeneration (AMD), Stargardt disease, and retinitis pigmentosa, are phenotypically diverse but can be treated with stem cell therapy (6,7). In the population above the age of 55, AMD is the leading cause of blindness worldwide. AMD affects 1.75 million people in the USA alone and will affect nearly 196 million people worldwide by 2020 (8).

Retinitis pigmentosa (RP) encompasses a heterogenous group of progressive retinal degenerative disorders with a worldwide prevalence of 1 in 3500–5000 individuals (9). Patients with RP typically present in later stages of the disease given that their central vision remains intact for a long time. These and many other currently untreatable retinal conditions are the subject of many clinical trials using embryonic stem cells (ESCs) and induced pluripotent stem cells (iPSCs) to treat these underlying conditions (10,11)

During retinogenesis, ESCs undergo a stepwise developmental process through primitive eye field (EF) and retinal progenitor cell (RPC) stages and then commit to neuronal and photoreceptor subtypes (12).

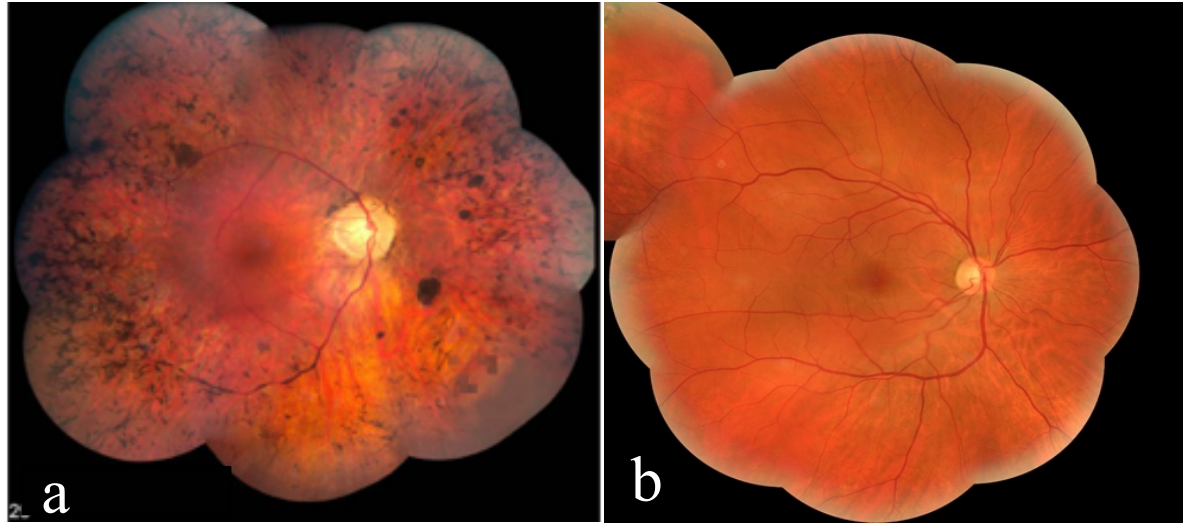Retinitis Pigmentosa and retinal stem cell Transplantation



**Figure 2-** Panel A: fundus photograph of a patient suffering from retinitis pigmentosa. In the areas with increased dark pigmentation photoreceptor death has occurred as the pigment in the underlying RPE is easily evident. Panel B is demonstrating a healthy retina for comparison.

Retinitis pigmentosa (RP) is an inherited disease which claims a person's vision over decades. There are still many unknown genetic mutations that can cause RP. It is difficult to develop a single specific gene therapy as patients afflicted with RP have an extensive disease causing genetic heterogeneity (13). Loss of functional proteins leads to disruption of normal photoreceptor cell structure causing cell death and irreversible blindness. As one example, Lamba et al. (14), transplanted retinal progenitor cell (RPC) suspensions into normal mice and mice with photoreceptor genetic defect. This experiment showed that the RPC could migrate and integrate into the various layers of the retina, but only if they were injected before the retinal degeneration began. A careful reading of the report reveals that transplanted RPC slowed the progression of the disease, but could not reverse the degeneration that had already occurred (13). The RPC graft suspensions fail when they are introduced into a diseased environment. By engineering the RPCs

into a flat tissue in which cell-cell interactions are already established, or by developing a homogenous photoreceptor cell population, the graft might survive and integrate with the remnants of the host tissue to restore lost vision.
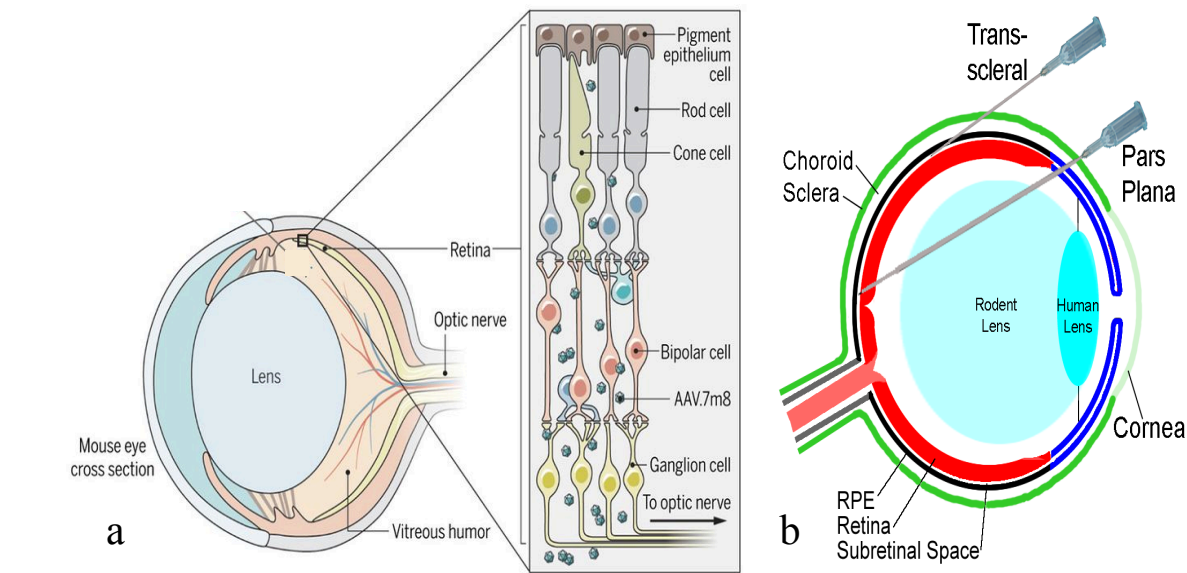
Planar retinal graft development



**Figure 3-** The illustration depicts the layered retinal anatomy and injection of stem cells into the subretinal space of the mouse eye using a trans-scleral approach given the lens is bigger in mice compared to human eyes. Panel a is adapted from 4a. Panel b courtesy of L. Rizzolo, Yale Univ.

The problem confronting the field is that the more mature assemblies of differentiated RPC cannot be transplanted for two reasons: The assemblies of retinal-like cells do not survive dissociation to single cells and injection into the subretinal space. The geometry of the cell assemblies is not amenable to transplantation. Depending on the protocol the cells form rosettes on a culture dish or neurospheres in suspension culture. The rosettes and neurospheres are of small diameter and would have to be converted to flat sheets in order to interact with the host retina and RPE. Accordingly, the only successful transplantation experiments involve suspensions of immature

cells in the earliest stages of retinal degeneration. Later investigators achieved some success in late stage disease using mouse models of retinal degeneration. Rod precursors were purified and the suspension was injected into the subretinal space after the photoreceptor layer degenerated. Success depended on the disease model that was used (15,16). Several labs have cultured RPC in sheets, but the scaffolds used would block interactions with either the host retina or the RPE (17,18). With designing a biocompatible scaffold that would foster differentiation of H9 embryonic stem cells (ESCs) it is possible to develop planar retinal structures.

Electrospun fibers of ε-polycaprolactone was tested in the Rizzolo lab in prior years. It did foster ESC differentiation into RPCs. However, it did not allow for full thickness migration (120 μm) of the cells through the scaffold. This prompted the Rizzolo lab to develop a porous scaffold made with hyaluronic acid, chondroitin sulfate and gelatin which closely resembles the retinal basement membrane composition. The gelatinous scaffold was used to differentiate the RPCs in a planar structure above the retinal pigment epithelium (RPE) layer. The differentiation of ESCs in the vicinity of RPE mimics the in vivo environment where photoreceptors are naturally developing. This contact with the RPE can help guide the differentiation of ESCs into photoreceptors in vitro.

There have been many established tissue culture methods that are used to differentiate RPCs into different retinal cells *in vitro*. A converging body of data has showed the ability of human embryonic stem cells (hESC) and induced pluripotent cells (hiPSC) to differentiate into neural retinal lineages and finally become photoreceptors and interneurons (19). However, to develop functional photoreceptor outer segments the RPE is required.  It is unknown if co-culture with RPE would induce synapse formation between the photoreceptors and interneurons to create a light-sensitive tissue. I will be using the RPE/RPC coculture method developed by the Rizzolo lab for developing the retinal graft.

Ongoing retinal stem cell transplantation clinical trials

ESC derived photoreceptor transplantation trials are still being completed. However, ESC derived RPE stem cell transplantation has been done. A landmark study of ESC transplantation done by Schwartz et al. showed that $5 \times 10^4$ ESC-derived RPE cells can successfully be transplanted into the eye of patients with age related macular degeneration (AMD) and Stargardt's macular dystrophy. Four years post transplantation, these Phase 1/2 clinical trials did not show signs of rejection, ectopic tissue or tumor formation, or hyperproliferation. (10). The ESC-derived RPE transplantation was done in 18 patients which confirmed long- term safety and graft survival. Patients tolerated the graft well and the adverse effects were mainly limited to the surgical procedure and oral immunosuppressive regimen. Even though the eye is considered to be an immune privileged organ the patients were on an oral immunosuppressive regimen given the cells were derived from ESC (20). At the end of the trial, there was minimal improvement in best-corrected visual acuity and quality-of-life measures. More tests such as microperimetry, auto fluorescence imaging, optical coherence tomography scanning, and multifocal electroretingram can be done to establish visual function (21). In order to reduce the need for oral immunosuppressive therapy, iPSC derived RPE can be used if the cells are obtained from the patient.

Preliminary mouse studies have grafted human iPSC-derived RPE cells into the subretinal space of mouse eyes. This study found that human iPSC-derived RPE cells restored some retinal function assessed by electroretinography in a mouse possessing the mutation in a gene known to be responsible for certain types of retinitis pigmentosa (RP) (22).

PDE6b is a protein that plays a key role in cGMP hydrolysis and photoreceptor hyperpolarization.

This protein is essential in converting all-trans retinol to 11-cis retinal during photoreceptor phototransduction and visual pigment regeneration (23).
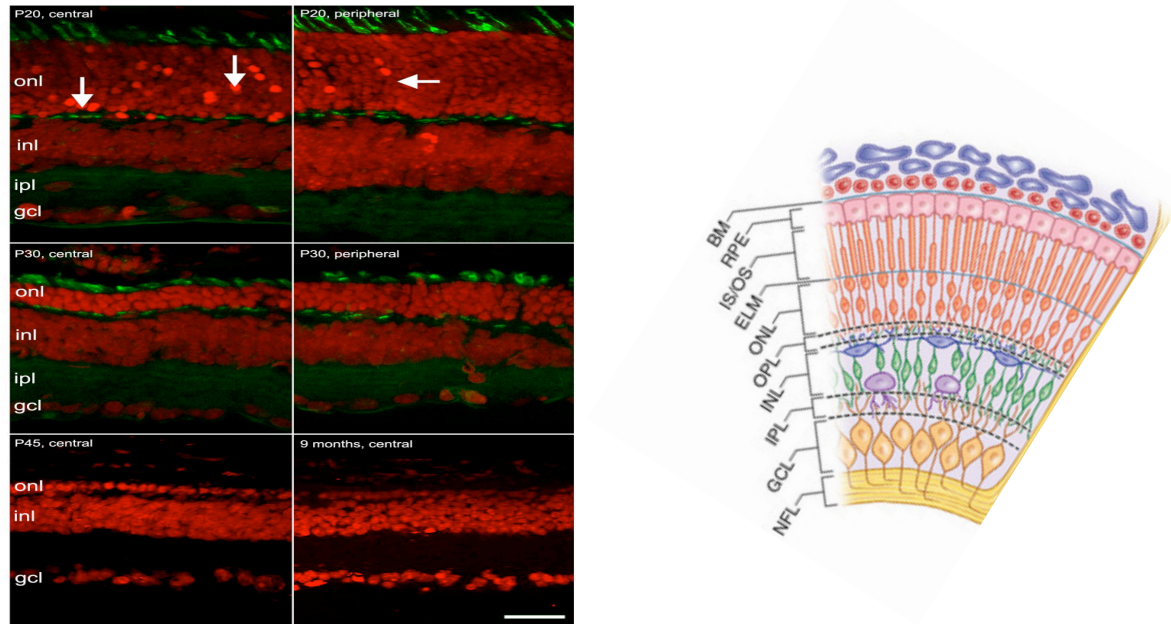


**Figure 4-** This panel demonstrates the RD10 mouse retinal histology over time. The outer nuclear layer (ONL) thinning, which corresponds to photoreceptor degeneration, is significant by day 30. Arrows are depicting actively dying photoreceptors. Figure adapted from Gargini C et. al Organization in the retinal degeneration 10 (rd10) Mutant Mouse (24).

To test retinitis pigmentosa (RP) reversal in vivo, I transplanted our engineered retina into RD10 mice, which has a PDE6b gene knockout. PDE6b KO causes degeneration of rod and cone photoreceptors and is also a gene that is linked to RP in humans and some cases of Leber congenital amaurosis (25). Notably, the RD10 mouse's phenotype causes the photoreceptor layer to degenerate from full thickness starting at 16 days until photoreceptors are nearly absent after 35 days after in the central retina.

**Statement of Purpose**

**Aim 1.** Develop a planar retinal graft on a gelatinous scaffold for in vivo transplantation of a homogenous RPC population or purified rod precursors for subretinal injection.

I hypothesize that development of a multilayered planar retinal graft will enhance the integration of RPCs into the injured photoreceptor layer and further differentiation into the photoreceptor lineage in vivo. Moreover, I want to compare the transplantation of the RPC/GCH graft to the injection of a homogenous photoreceptor cell suspension in the subretinal space.

**Aim 2**. Evaluate the side effects of RPC graft/scaffold transplantation such as tumergenicity, uveitis, retinal edema, inflammatory response and retinal scaring.

I hypothesize that since the scaffold is mostly made of gelatin, hyaluronic acid, and chondroitin sulfate and roughly resembles the matrix of the retina that the inflammatory response will be minimal and the scaffold can be degraded in vivo. Also the since the scaffold is implanted in the subretinal space, which is immune privileged, inflammatory response is minimum.

**Aim 3.** Transplantation of in-vitro differentiated RPC into a retinitis pigmentosa mouse models at the intermediate and late stages of disease.

I hypothesize that RPCs can migrate towards the layer of injury and will integrate in the photoreceptor layer in the retinitis pigmentosa mouse model given the photoreceptor layer has undergone 90% degeneration by P30.

**Materials and Methods**

C57/BL6 mice and RD10 mice were used at P30. All experiments were done in accordance to ARVO statement for the use of animal in ophthalmic and vision research. Gelatin powder was purchased from J.T.Baker, New Jersey (USA). Chondroitin sulfate, 90+% and hyaluronic acid was obtained from Alfa Aesar, MA (USA). Ammonium persulfate by fisher scientifics, New Jersey (USA). N,N,N',N'-Tetramethylethylenediamine, Tri-Buffer-saline with 1% tween 20, Phosphate buffer saline (PBS) 1X , pH 7.4 containing 1.4M NaCl, 0.1M phosphate (pH 7.4) and 0.03M KCl were all purchased from American BIO, MA (USA). Glutaraldehyde, 50% Ameresco, Ohio (USA). Milli-Q-grade water was used in all experiments except for gene expression in which nuclease free-water from Bio-rad. i-Script cDNA synthesis kit, iTaq$^{tm}$ Universal SYBRGreen Supermix and PCR plates were purchased from Bio-rad, Hercules (USA). All the solvents used here without any further purification were purchased from Sigma-Aldrich.

Preparation of 3D scaffold

Different combination of polymers was used to fabricate the gelatin-chondroitin sulfate-hyaluronic acid (GCH) scaffold. 250mg of gelatin, 125mg of chondroitin sulfate and 250mg of hyaluronic acid were dissolved in water. 50 µl of glutaraldehyde cross-linker with reaction initiator ammonium-persulphate and redox catalyst *N,N,N',N'*-tetramethylethylenediamine (TEMED) catalyst, were added to the dissolved solution. Polymer solution was frozen at -20 °C for 18 hrs and vacuum dried using lyophilizer to produce a solid 3D scaffold. Scaffolds which were mechanically stable enough were frozen in OCT and sectioned using a cryotome to a 60µm thickness.

Human Embryonic stem cells (H9) culture maintenance and differentiation

Undifferentiated H9 human embryonic stem cells were obtained from the Yale stem cell center. Cells were cultured on 1% matrigel coated plates and maintained in mTeSR-1 media. Media was changed every 2 days and colonies were regularly scraped under a sterile microscope to remove spontaneously differentiating cells. For passaging, colonies were lifted by incubating with 1U/ml dispase for 30 min at 37˚c, triturated and washed with DMEM/F-12 nutrient media and plated onto newly 1% matrigel-coated dishes.

For the RPC differentiation process, H9 cells were treated with blebbestatin following the dispase step in order to make embryoid bodies (EBs). EBs were cultured in mTeSR-1 at D0. Neural induction medium (NIM) containing B27 was added the next day (D1) in a ratio of 1: 3 with mTeSR-1. On D2 the concentration of NIM increased to 1:1 with mTeSR-1 and on D3 and onwards EBs were cultured in 100% NIM. On D7 the floating EBs were seeded on matrigel coated 6 well plates and continued to be cultured in NIM until D20. The retinal progenitor cells (RPC) were selected and manually dissected out from the plates for further experimentation.

EBs on GCH scaffold seeding for retinal cup differentiation

EBs formed using H9 were seeded onto GCH scaffold on D20. Scaffolds were sterilized overnight with 70% ethanol, washed three times with PBS, then treated with pen-strep for 30 mins and soaked in NIM overnight. 6-8 EBs were seeded on the scaffold the following day. Media was changed 2 to 3 times a week until retinal cup formation was visually observed.

## Immunofluorescence Confocal microscopy

from D20 onwards, each week seeded scaffolds were collected to observe for cellular migration and differentiation using confocal microscopy. Scaffolds were fixed in 4% paraformaldehyde for 5 mins following wash with cold PBS. Scaffold was placed in OCT fluid and cryotome sectioned and placed on glass slides. Sectioned H9-GCH scaffolds were permeabilized with 0.1 Triton-X for 60 mins. 10% donkey serum containing 0.1% Triton-X solution in PBS was used to block the samples for 1 hr. Next, the sections were incubated overnight with primary antibodies (listed in table 2). The slides were washed three times with PBS and blocked again for 1 hr with 10% donkey serum in order to reduce background fluorescence before incubation with secondary antibodies conjugated with Cy2, Cy3, or Cy5 (Jackson ImmunoResearch Laboratories, West Grove, PA). DAPI (4,6-diamidino-2-phenylindole) was used to label the nucleus. Before mounting the slides, sections were washed three times with PBS and fluorescence images were captured with an LSM 410 spinning-disc confocal microscope and processed using Zen software (Carl Zeiss, Inc, Thornwood, NY). Images used are representative of 3 or more experiments.

## Electron Microscopy

EB seeded scaffolds were fixed in 4% paraformaldehyde. Further fixation was done by immersing the tissue in 1 % osmium tetroxide for 90 min. Samples were then dehydrated with a graded series of ethanol (50–100 %) baths, cleared in propylene oxide, and embedded in epoxy resin. Ultrathin sections were cut with an ultramicrotome and stained with uranyl acetate and lead citrate. Stained sections were then examined with transmission electron microscopy.

Quantitative Real-time RT-PCR

Total RNA was extracted using TRIzol reagent (Invitrogen, Paisley) according to manufacturer's instructions. cDNA was reverse transcribed using 2μg of total RNA using QuantiTect Reverse Transcription kit (BioRad). Quantitative reverse transcription polymerase chain reaction qRT-PCR was synthesized using iTaqSYBR Green (BioRad) and RNA primers generated at Keck Oligonucleotide synthesis facility (Yale University). Following positive expression, samples were further tested using customized PCR array for 48 genes specific to early eye field, neural retinal development, ganglion cells, terminal differentiation of photoreceptors, interneurons and retinal pigment epithelium lineage. Relative mRNA expression was normalized with housekeeping genes (GAPDH and Actin) and calculated using $2^{-\Delta\Delta Ct}$ method.

FACS sorting

Differentiating EBs were transfected with the AAV vector carrying the rhodopsin promoter upstreams of a Tdtomato sequence, which is a red fluorescent protein, 48 hours prior to flow cytometric cell sorting (FACS). EBs were dissociated with 0.25% trypsin for 15 min and Serum free media was added to inactivate the trypsin. Cells were spun down at 1000 rpm and strained to obtain a single cell suspension. Analysis was performed using the FACS Calibur system (BD Biosciences).

AAV virus preparation

293FT cell line was maintained with DMEM and 10% FBS and passaged 1:4 every 2 days. The 293FT cells were cultured in 150mm dishes. The media is changed when the cells are ready for

transfection (more than 70% confluent). For every 5x150mm culture dish the vector mix was prepared with 30 µg AAV vector; AAV rep/cap 50 µg;  adenol helper 60 µg.  The plasmid is mixed with 600 µl PEI (1µg/µl) to DNA mixture, vortexed and incubated for 25 min at room temperature. 120µl is added to each plate and cells harvested 48-72 hours post transfection. Collect cells using centrifugation at 1000g for 10 mins. Cell pellet was resuspended in 6 ml lysis buffer (150 mM NaCl, 20 mM Tris-HCl pH 8.0).  Cells were lysed using subsequent incubation in dry ice/ethanol mixture and 55 C water bath. 250U/Benzonase was added and incubated at 37C for 1 hour while vortexing every 15 mins. Cell lysates are centrifuged at 4000 rpm for 30 min and supernatant is filtered with a 0.45um syringe filter. The HiTrap heparin columns are setup with a 10 ml syringe and flow is kept below 1ml/mins. The column is equilibrated with 10 ml lysis buffer (150Mm NaCl, 20Mm Tris-HCl Ph8.0). The viral solution is passed through the column slowly. The column is washed with 3 ml 200Mm NaCl, 20Mm Tris-HCl Ph8.0, and 3ml 300Mm NaCl, 20Mm Tris-HCl Ph8.0 respectively. The virus is eluded with 1.5ml 400Mm NaCl, 20Mm Tris-HCl Ph8.0 and concentrated with Amico ultra-4 centrifugal filter units, and washed the collection with DPBS. Finally, aliquoted the concentrated virus and stored in -80C.

Animal experiment

All animal experiments were performed in accordance to the guidelines set and approved by Institutional animal care and use committee (IACUC) at Yale University, New Haven, CT. A total of two breeding pairs were required to complete this experiment. This pair was used for breeding and pups obtained were used for the implantation study. Wild-type and rd10 mice at post-natal day 30 were used for transplantation and following the completion of experiment mice were euthanized by prolong exposure to $CO_2$ followed by secondary form of euthanasia (lung puncture).

## Wild-type and RD10 mice implantation

For transplantation of GCH scaffold alone or scaffold with differentiated retinal cup tissue, the scaffold grafts were cut into 0.5 cm dimension and kept in PBS solution. Mice were anesthetized by intramuscular injection of a mixture of ketamine (100 mg/kg) and xylazine (10 mg/kg). A small scleral hole was made after conjunctival incision and a local retinal detachment was induced by PBS injection.  Subsequently, the scleral incision was enlarged. The small piece of scaffold was carefully inserted into the dorsal quadrants of the host retinas. After transplantation, the mice were transferred into a dark room for 1-2 days, and then maintained in regular animal facility.

## Statistical analysis

All data presented in this manuscript is shown as the mean $\pm$ standard deviation (SD) unless otherwise indicated. All experiments presented here were completed in biological and technical triplicates. The data from the experimental sets were compared with controls and statistical analyses was performed by one-way ANOVA, and p values <0.05 were considered statistically significant.

**Results**

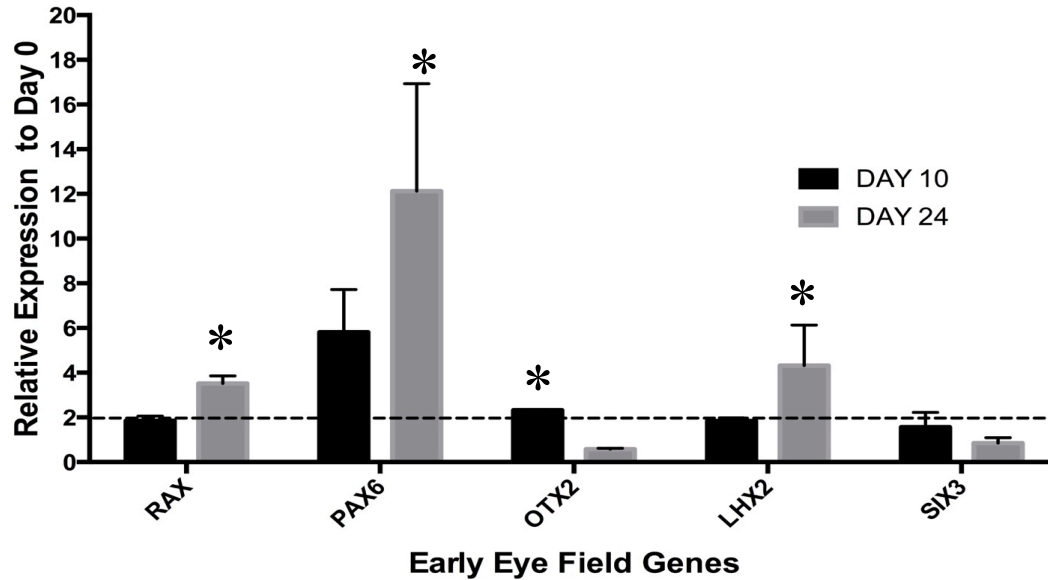Retinal Progenitor Cell Differentiation on GCH scaffold



**Figure 5-** qRT-PCR was done for monitoring neural retinal maturation on the gelatin scaffold. Dashed Line: 2X increase vs Day 0. qRT-PCR results are averaged from n=3 separate experiments. Statistically significant results are marked by asterisk.

The qRT-PCR analysis showed an increase in the expression of neural and early eye field genes of neurospheres on the GCH scaffold from D10. LHX2 shows a 6-fold increase on D24 compared to D0. On further testing at D10 and D24, PAX6 expression increased two-fold in comparison to D10. RAX and LHX2 increased 2-fold (Fig. 5) indicating the EBs on GCH scaffold were differentiating into RPCs. H9 cultured on GCH shows upregulation of important eye field transcription factors (RAX, SIX3 and OTX2), photoreceptor genes as evident on Fig. 5.

Immunofluorescence and confocal microscopy of RPCs also shows the upregulation of OTX2, SOX1 and RAX on D7 as expected. There is also a clear expression of RAX, PROX1, LHX2 at

D21 which are early eye field genes (Fig. 6). The expression of these markers was comparable to floating EB cultures which were used as a control.
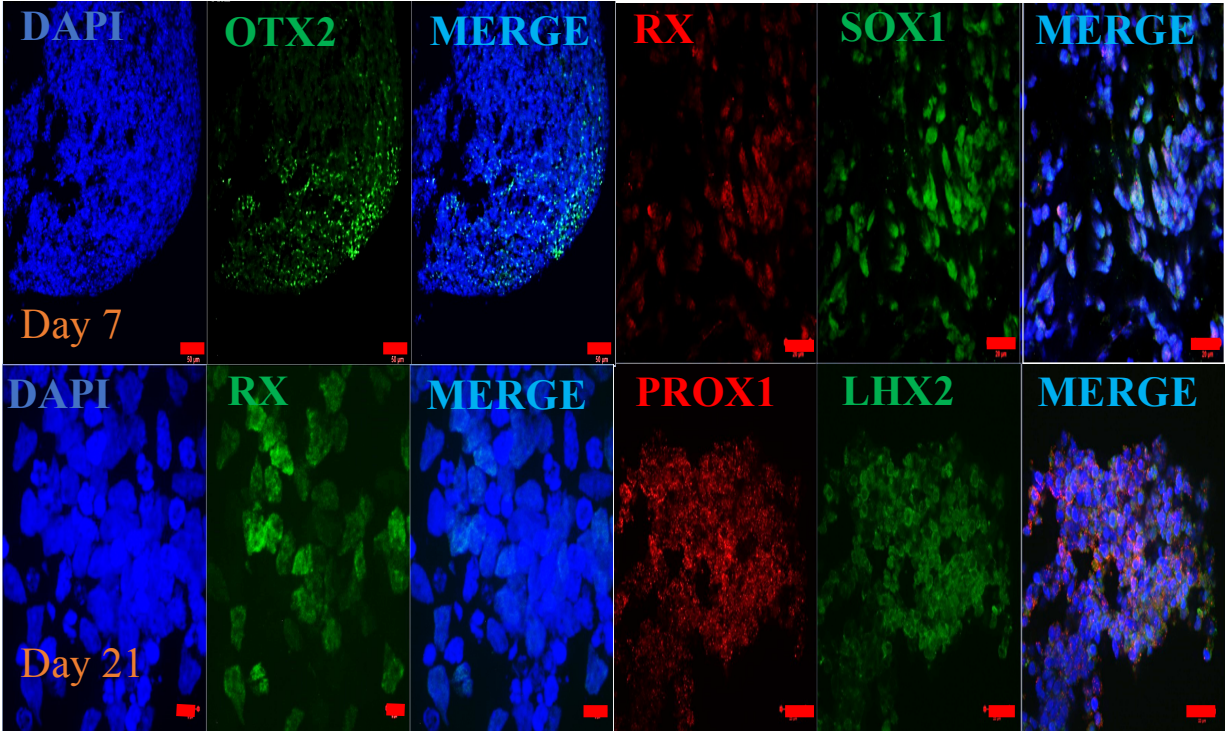


**Figure 6-** Confocal microscopic imaging of H9 differentiation in vitro, shows stepwise expression of early eye field proteins from Day 7 to D21 using immunohistochemistry. Bar 20μm.

Retinal Progenitor Cell interaction with GCH Scaffold

The final GCH fabrication product resulted in a homogenous scaffold with pore sizes ranging from 150-190 μm (Fig. 7 A, B). H9-GCH interaction was confirmed using bright-field and scanning electron microscope. EBs adhered to the surface of the scaffold (Fig. 7D) and maintained the EB morphology with a slightly polarized appearance, and some EBs contained the pigmented RPE which is consistent with differentiation towards a self-organizing neuro-epithelial lineage (Fig 7D). 2 weeks after the EBs were seeded onto the GCH scaffold, DAPI staining was done to assess

cellular migration within the scaffold. Confocal microscopy revealed that H9 cells attached, proliferated and migrated through the 60μm-thick scaffold (Fig. 7 E and C).
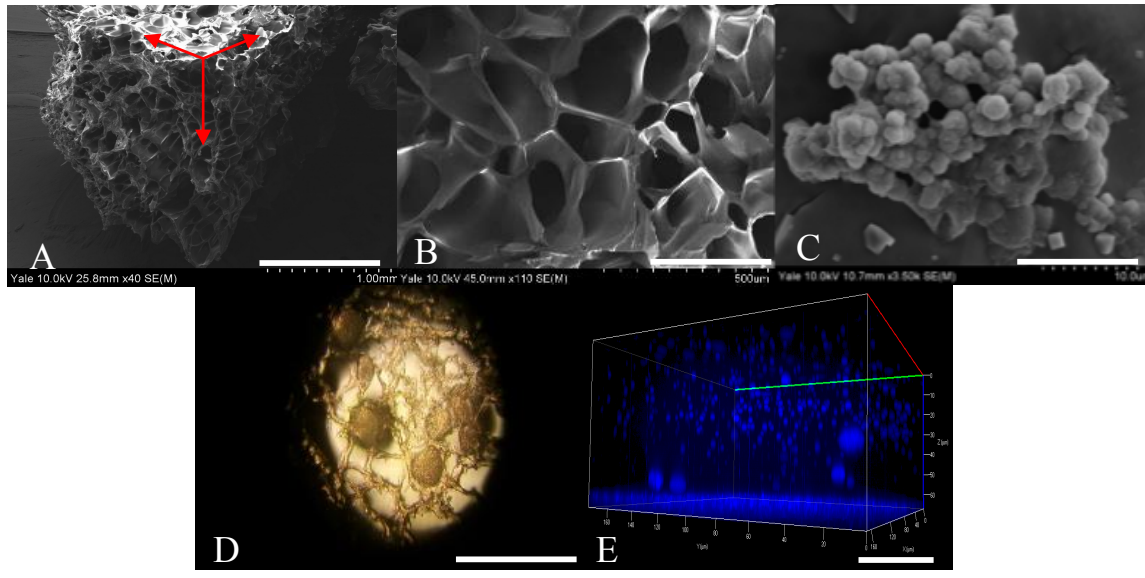


**Figure 7- A)** Scanning electron microscopy (SEM) image showing macroporous structure of the scaffold in 3D, **B)** and 2D view, (scale bars 1.00 mm and 500μm respectively) **C)** Human embryonic stem cells (H9) seeded onto gelatin scaffold D20 (scale bar 100μm). **D)** ESCs completely infiltrate two weeks after scaffold seeding on BF microscopy. **E)** ESCs migrate through the scaffold thickness (3D view) on confocal imaging. Scale bars 20μm.

RPC differentiation on GCH scaffold with RPE co-culture

RPCs differentiating on the GCH scaffold were placed on RPE that was cultured on transwell filters at D20. The differentiation process continued in proximity to the RPE mimicking in vivo conditions. Samples were taken on D90 and immunofluorescence showed a discrete separation between recoverin positive cells and LHX2 positive cells as seen in Fig. 8. There was 7-8 rows of recoverin positive cells adjacent to the RPE layer which is the location of photoreceptor development in vivo.
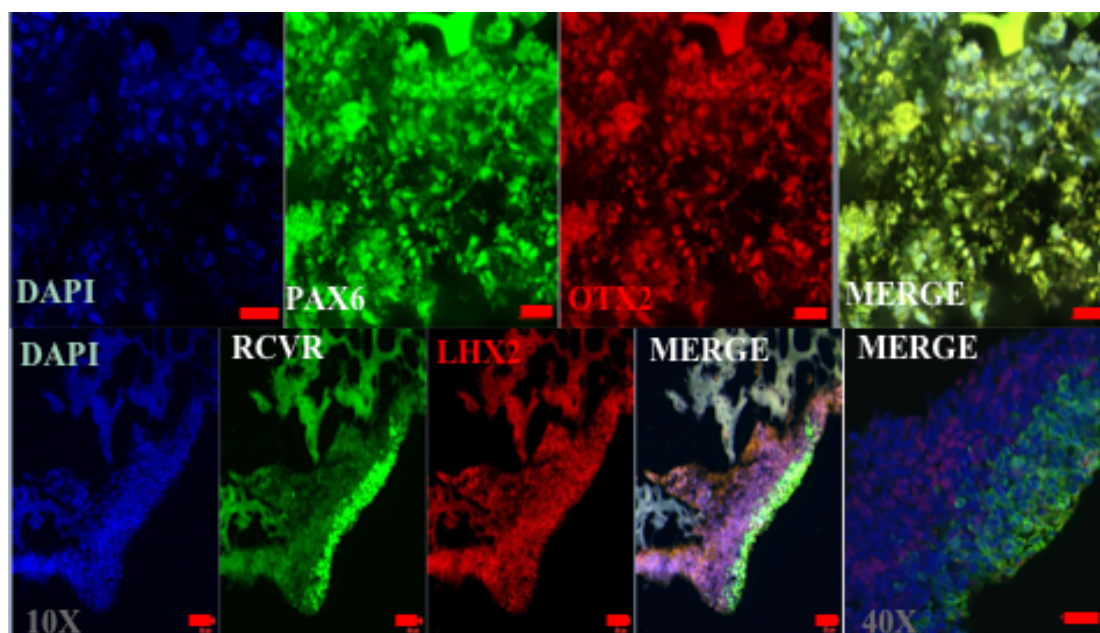
**Figure 8-** The upper panel Represents confocal imaging of H9 cells on the GCH scaffold expressing early eye field proteins at D40 (scale bar 20µm). The lower panel demonstrates ESC differentiation in proximity to RPE cells at D90 (scale bar 50µm). Besides migrating into the scaffold, cells proliferate as broad flat clusters on the scaffold and recoverin positive cells (green) segregate from LHX2 positive (red) cells. The recoverin positive cells matured proximal to the RPE. (Note that the scaffold is autofluorescent and appears in multiple channels.)

Biocompatibility of RPC/GCH transplantation in wild type mice

To investigate the in-vivo response to RPC-GCH, the scaffold was implanted in the subretinal space of wild type and RD10 mice. Three weeks post transplantation, the RPC-GCH scaffold biocompatibility and host inflammatory response was evaluated by IL-6 detection levels in the tissue. IL-6 staining was found to be minimal at the site of implantation and around the scaffold in both wild-type and RD10 mice (Fig. 9). In wild-type mice transplanted with RPC-GCH, some IL-6 positive staining was found in and around the area of the choroid which is where IL-6 positive

cells are physiologically present (Fig. 9). However, minimal IL-6 positive cells could be seen at the site of implant (Fig. 9). There was minimal host inflammatory response to the transplanted scaffold. Most of the scaffold was degraded 6 weeks post transplantation (figure not shown).
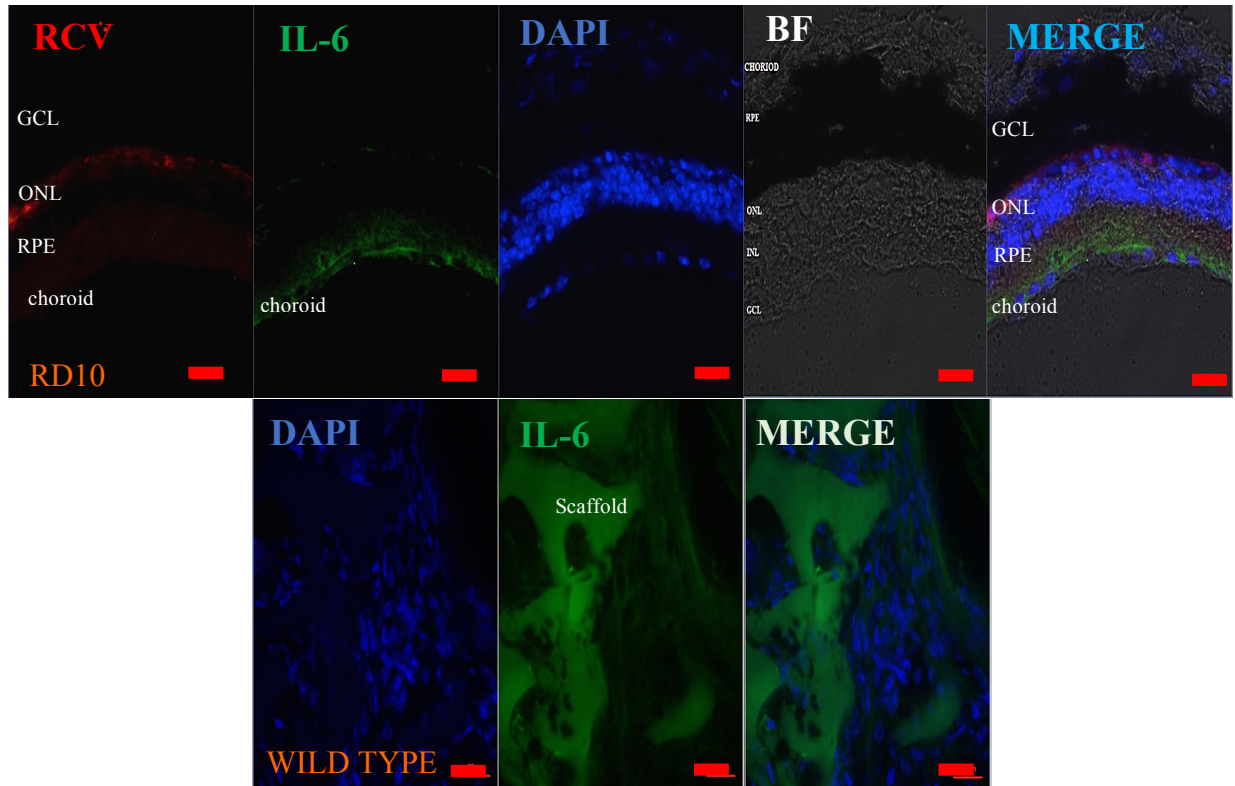


**Figure 9-** Confocal image of wild type retina 3 weeks post implantation of RPC on GCH scaffold. IL-6, a major inflammatory marker, was used to demonstrate host response to scaffold. In both panels there is minimal expression of IL-6 noted suggesting the biocompatible nature of the fabricated scaffold. IL-6 is seen in the choroid layer in RD10 panel where it is usually seen in vivo. Scale bar is 20μm.

Migration of transplanted RPC on GCH into host retina

Immunohistochemistry examination of the RPC-GCH implant in the sub-retinal space of wild type mice 6 weeks after implantation shows minimal inflammation and migration of human antigen positive cells (TRA-1-85) into other retinal layers of the mice (Fig 10). The TRA-1-85 positive staining is showing the retinal vascular pattern as the antibody cross reacts with mouse blood cells

that failed to be removed by saline perfusion post euthanasia. In wild type mice, migration is minimal unless ONL is diseased or injured. TRA-1-85 positive cells were found within the transplanted scaffold showing that the RPCs are viable within the GCH scaffold after transplantation.
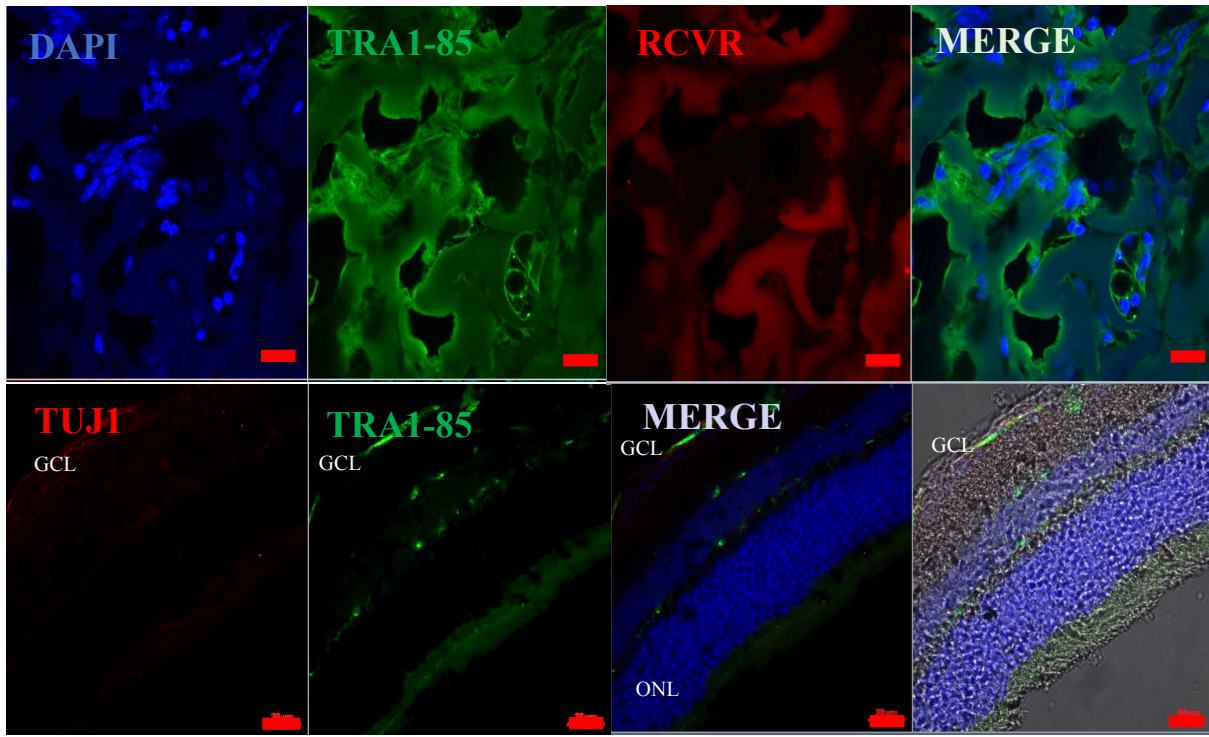


**Figure 10**- RPC/GCH scaffold implants in WT mouse 3 weeks post transplantation. The cells within the scaffold are positive for human antigen TRA1-85, which shows that mouse cells did not invade the scaffold in the subretinal space. Some TRA1-85 positive cells show vasculature pattern in the different layers. RPCs do not migrate when there is not a layer of injury. Bar, 20μm.

6 weeks post transplantation of GCH/Scaffold in RD10 mice showed the scaffold had been resorbed. However, RPCs were seen to migrate and adhere to the host retina, adding an extra layer of cells in the outer nuclear layer (Fig 11). In the ONL there is a layer of TRA1-85 positive cells adjacent to a row of recoverin positive cells. TRA-1-85 positive cells were seen to extend their cellular processes and migrate deeper into the ONL layer (Fig. 11) indicating that the implanted RPC were able to survive transplantation stress, and migrate into the degenerating photoreceptor

layers. To further confirm cellular migration and attachment of RPC into the ONL layer, samples were co-stained with recoverin and TRA-1-85 showing a distinct layer of TRA-1-85 positive cells on top of the homogenous recoverin positive photoreceptors in the ONL (Fig. 11).
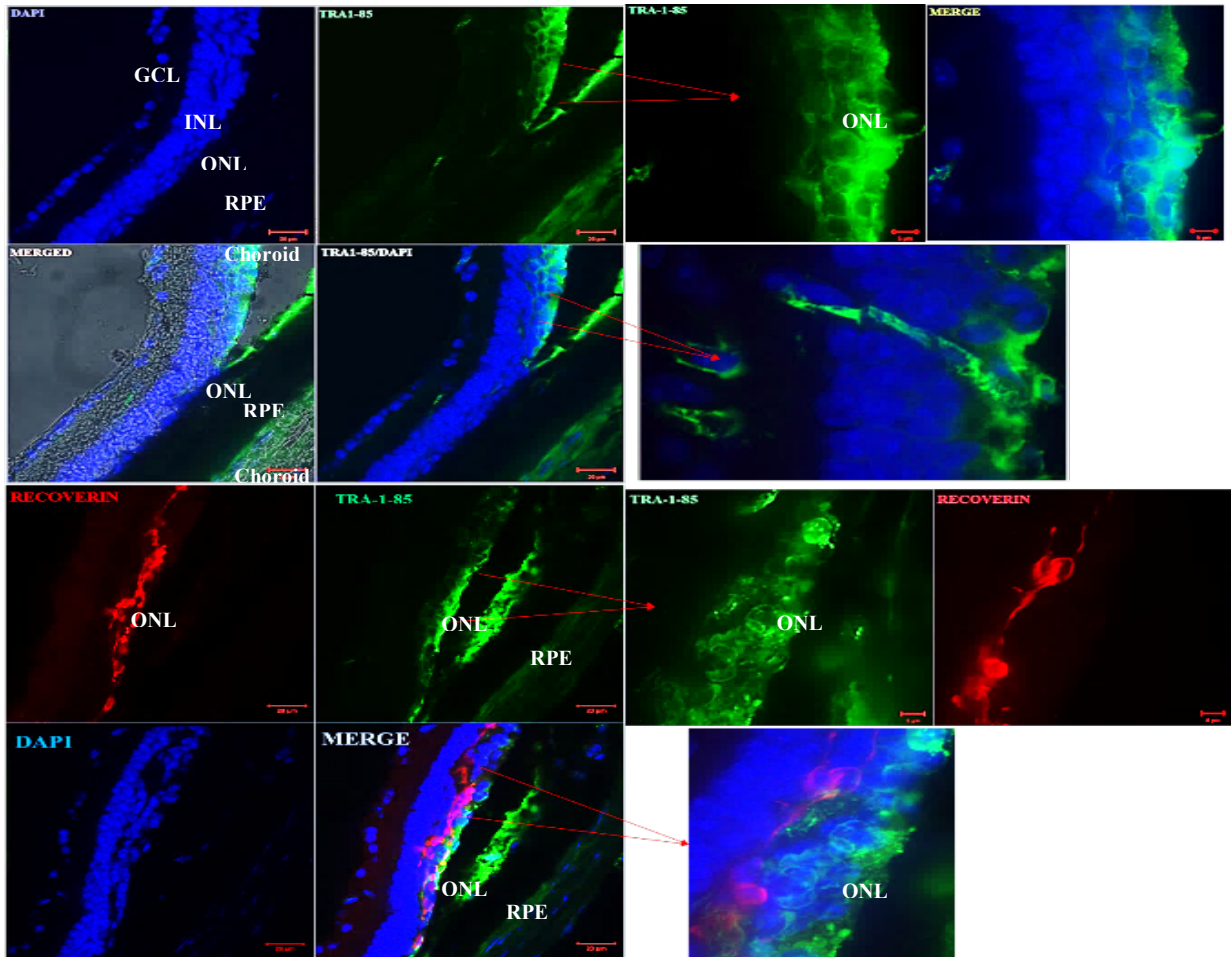


**Figure 11-** Confocal images the 6th week post implantation. TRA-1-85 (green), recoverin (red) and DAPI (blue) cells were found to integrate with the host photoreceptor layer. Recoverin staining was performed to confirm the retina orientation. The panel shows TRA-1-85 positive cells at site of implant. The transplanted cells do not express recoverin. At 6 weeks there is clear attachment of human antigen positive cells at the site of implantation both at the ONL and RPE layers. Scaffold degraded within the 6th week of implantation allowing migration and integration of grafted cells into host retina. Figure curtesy of Deepti Singh, Yale Univ.

FACS Sorting of Rho + transfected RPCs and subretinal injection in RD10 mice

Some cells were lost in the process of developing a single cell suspension for FACS given the

longer exposure to trypsin in order to break up the neurosphere. 20% (2x $10^5$ cells) of the RPCs

were expressing rhodopsin, which is expressed in photoreceptors (Fig. 12).
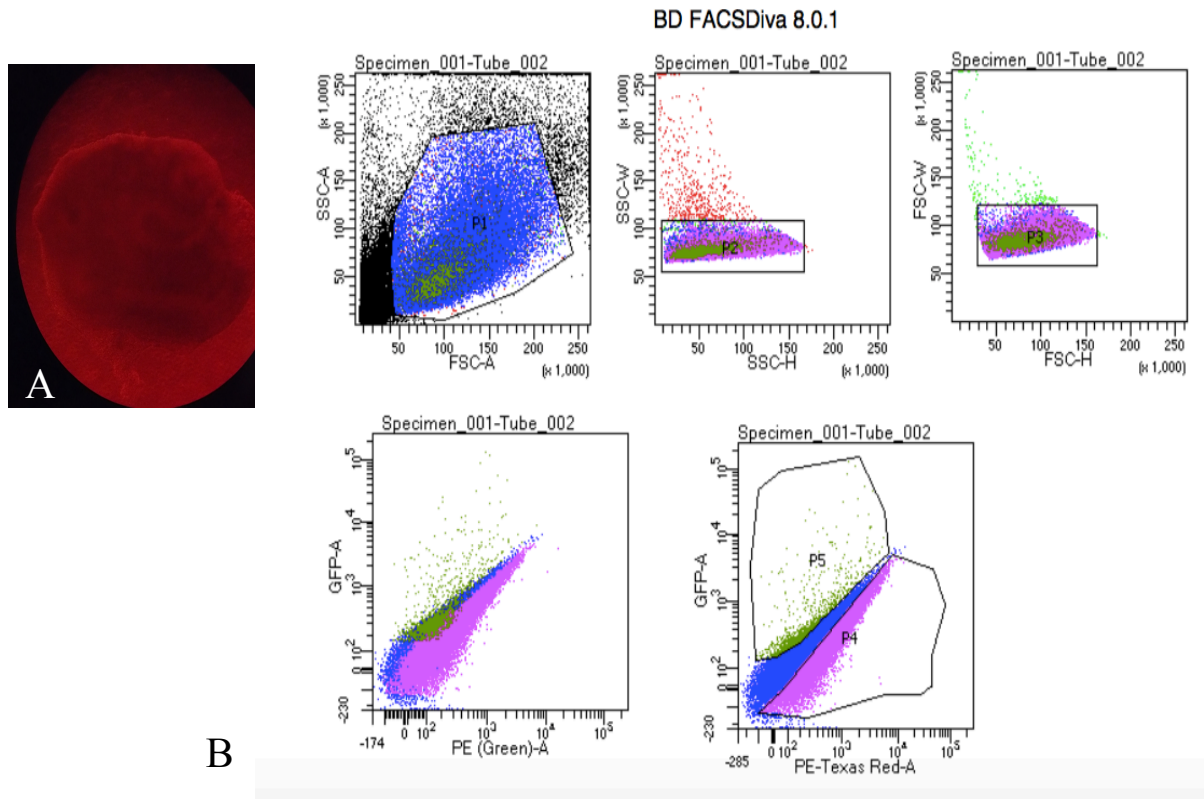


**Figure 12-** FACS sorting neurospheres transfected with Td/tomato Rho+ AAV. Photoreceptors generally differentiate in the periphery which will express rhodopsin at D50. Panel A shows rhodopsin positive cells in the periphery. Panel B demonstrates a distinct population of Rho+ cells in P4 which will be used to for subretinal injection in RD10 mice.

50,000 cells were injected in one eye of the RD10 mouse. Ku-80 Immunofluorescence, which is

an antibody marking human antigens, shows the presence of a homogenous photoreceptor

population in the subretinal space 3 weeks post injection. The cells were viable and intact through

the injection process. There was also minimal inflammatory response, given the minimal IL-6 was observed on immunofluorescence (Fig. 13).
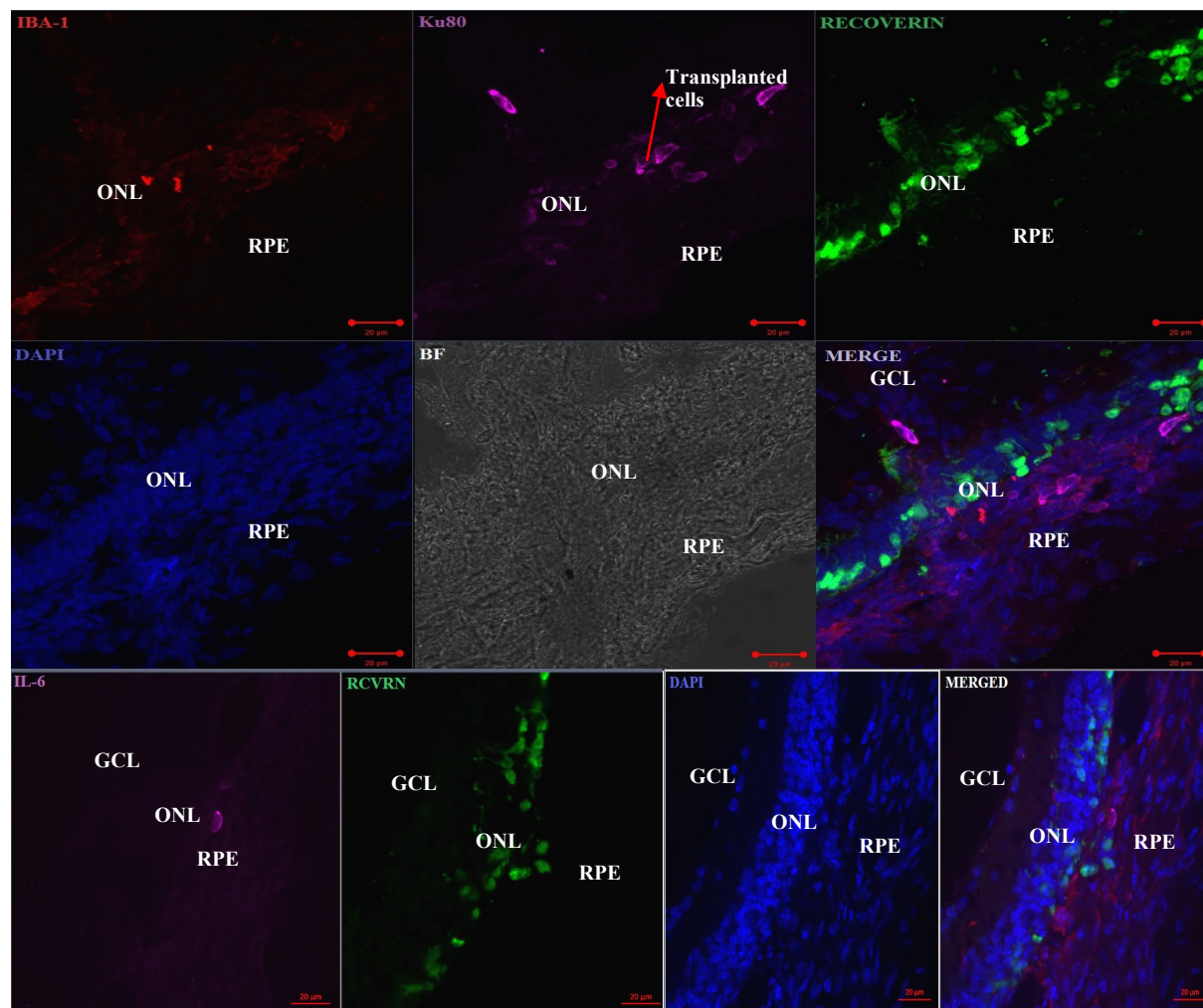


**Figure 13-** Subretinal injection of FACS sorted Rho+ cells in the subretinal space of RD10 mouse at P30. Confocal images are 3 weeks post-injection. Ku80 is an antibody against human antigens. The host cells express recoverin while the injected cells are only Ku-80+. IL-6 staining shows minimal inflammatory response in the lower panel. The layer labeled "RPE" includes the underlying choroid.

## Discussion

Methods of cellular delivery and survival rate for transplantation has been a technical challenge in regenerative medicine. The layered and flat retinal anatomy poses a specific challenge for stem

cell delivery given current stem cell differentiation protocols result in spherical eye cup structures (26). The gelatin-chondroitin sulfate-hyaluronic acid scaffold approximates the retinal extracellular composition (27). Gelatin was substituted for collagen, because it is less immunogenic than the collagen from which it is derived (28). I have shown that the H9 ESCs differentiate readily on the GCH scaffold compared to the control floating embryoid body cultures. Early eye field genes such as RAX, LHX2, PAX6, and OTX2 are upregulated as evident by qRT-PCR results, immunofluorescence and confocal microscopy. The ESCs migrate through the 60μm thickness of the scaffold given the interconnected scaffold pore morphology constructed through rapid freezing and drying using a lyophilizer. Since EB's are large cell clusters, it is difficult for most clusters to achieve complete migration in a 3D structure. However, the macroporous interconnected pores of GCH showed the possibility of attaining 3D cellular growth. The GCH scaffold was superior in supporting RPC formation and ESC differentiation in comparison to PCL scaffolds previously studied in the Rizzolo lab. ESCs were mostly aggregated on the surface of the PCL scaffold given the scaffold did not have the porous structure as the GCH scaffold. Currently, the members of the Rizzolo lab have found that GCH coating with laminin 521 further enhances RPC attachment, migration and differentiation.

The RPC/RPE coculture experimental samples clearly formed a planar retinal structure with recoverin positive cells differentiating adjacent to the RPE layer. These samples were fixed for immunofluorescence on D90 of the differentiation protocol. These samples were not used for transplantation studies given the scaffold was partially degraded in culture and did not have the mechanical stability to be used in animal studies. The scaffold partially degrades when is placed adjacent to the RPE, possibly due to metalloproteinase secretion by the RPE.

The scaffold causes minimal host inflammatory response when transplanted in both wild type and RD10 mice, as there is minimal IL-6 detected on immunofluorescence and there is no retinitis seen in mice post transplantation. There is no increase in IBA-1 or IL-6 positive cells at the site of implant or within the vicinity of the scaffold. Few IL-6 positive cells were detected in the photoreceptor layer in both wild type and RD10 mice at the 1st week post transplantation could be due to surgical procedure or host response to the graft. However, in the later stages absences of both types of cells indicates the graft was well tolerated by the host and does not cause a major inflammatory response.

The GCH scaffold is mostly degraded at 6 weeks post transplantation, however there is a retinal detachment at the site of transplantation when the scaffold is degraded. The retinal detachment is caused by the volume of the transplanted scaffold in comparison to the mouse subretinal surface area. The RPCs are viable within the scaffold when transplanted and there is no invasion of host cells into the scaffold as evidenced by the presence of TRA1-85, a human antigen marker, seen on immunofluorescence within scaffold pores.

There is RPC integration within the RD10 outer nuclear layer, which is the site of photoreceptor loss and injury, 6 weeks post transplantation when the RPC/GCH graft is transplanted. It is thought that RPCs migrate and home to the site of injury within the retina. This integration is more notable when the RPCs on the scaffold are transplanted on D20-D24 of differentiation. During that timeline the cells are in the progenitor state and are more capable of differentiating into different retinal cells and integrating and further differentiating at the injury site.

FACS analysis of RPCs was done on D50 of the differentiation protocol after transfection with rhodopsin positive AAV. FACS sorting of $1 \times 10^6$ RPC cells transfected with Rho+ AAV yielded

only $2x10^5$ Rho+ cells.20% of the RPC population was expressing rhodopsin which is present in the later stages of photoreceptor differentiation.

The injection of 50,000 Rho+ cells in the subretinal space of RD10 mice resulted in a viable homogenous photoreceptor cluster in the subretinal space 3 weeks post injection. There was a few Ku-80+ cells, which is a human antigen marker, seen in the outer nuclear layer. However, it is unclear if these are the injected human cells which have migrated and integrated in the ONL or the remaining mouse photoreceptors have taken up the marker through cytoplasmic exchange (29). In that event, it would appear the transfer of mRNA to host cells had a protective effect. The transcleral injection of Rho+ cells causes minimal inflammation given there is only one IL-6 positive cell detected at the injection site. The injection does not seem to have disrupted the retina blood barrier. Integration of rhodopsin expressing photoreceptors into the ONL might be more difficult, given these cells are almost mature photoreceptors.

Cells in the RPC (differentiation day 20-24) stage can theoretically integrate more readily as evidenced in Fig. 12 in comparison to more mature RPCs this finding could be explained by the fact the retinal cups start forming during the D20-D24 timeframe and most of early eye field genes are expressed within this earlier window. It might be difficult for cells to migrate after complete commitment to a specific retinal lineage such as in the rhodopsin+ FACS sorted cells transplantation experiment. For this reason, the Rizzolo lab has acquired a GFP+ SIX6 expressing ESC line. SIX6 is an early eye field gene, and marks RPCs in an early differentiation stage. The SIX6+ stem cell population can be cell sorted and used to seed the GCH scaffold for further transplantation studies or subretinal injection studies.

Retinal functional recovery evaluation post transplantation will be done using multifocal electroretinogram (mfERG) studies at the site of transplantation. However, in order to achieve any

measurable functional recovery, it is hypothesized that at least 150,000 RPCs must integrate in the ONL layer in photoreceptor degenerative diseases (30). The lab is currently working on achieving a reliable method to perform mfERGs on the mouse models.

**Conclusions**

The GCH scaffold supported the differentiation and attachment of RPCs. The RPC/RPE co culture resulted in a polar planar retinal structure with recoverin expressing cells adjacent to the RPE layer.

In this study, we found significant amount of cells migrated into the photoreceptor layers within 6 weeks when RPC-GCH was implanted on differentiation days 20-24. Less integration was seen when a homogenous photoreceptor population was injected in the subretinal space at a later differentiation time point. Furthermore, the scaffold was mostly degraded within the 6-week time frame without altering the retinal architecture or causing any immune rejection. However, there was a retinal detachment at the site of scaffold transplantation.

# Reference

1) H. P. N. Scholl, R. W. Strauss, M. S. Singh, D. Dalkara, B. Roska, S. Picaud, J.-A. Sahel,

Emerging therapies for inherited retinal degeneration. Sci. Transl. Med. 8, 368rv6 (2016).

2) A. J. Smith, J. W. Bainbridge, R. R. Ali, Prospects for retinal gene replacement therapy.

Trends Genet. 25, 156–165 (2009).

3) A. Rattner, H. Sun, J. Nathans, Molecular genetics of human retinal disease. Annu. Rev. Genet. 33, 89–131 (1999).

3a) A. V. Cideciyan, S. G. Jacobson, W. A. Beltran, A. Sumaroka, M. Swider, S. Iwabe, A. J. Roman, M. B. Olivares, S. B. Schwartz, A. M. Komáromy, W. W. Hauswirth, G. D. Aguirre, Human retinal gene therapy for Leber congenital amaurosis shows advancing retinal degeneration despite enduring visual improvement. Proc. Natl. Acad. Sci. U.S.A. 110, E517–E525 (2013)

4) Petrs-Silva, A. Dinculescu, Q. Li, W.-T. Deng, J.-J. Pang, S.-H. Min, V. Chiodo, A. W.Neeley, L. Govindasamy, A. Bennett, M. Agbandje-McKenna, L. Zhong, B. Li, G. R. Jayandharan, A. Srivastava, A. S. Lewin, W. W. Hauswirth, Novel properties of tyrosine-mutant AAV2 vectors in the mouse retina. Mol. Ther. 19, 293–301 (2011).

4a) G. H. Travis, M. Golczak, A. R. Moise, K. Palczewski, Diseases caused by defects in the visual cycle: Retinoids as potential therapeutic agents. Annu. Rev. Pharmacol. Toxicol. 47, 469–512 (2007)

5) D. Dalkara, L. C. Byrne, R. R. Klimczak, M. Visel, L. Yin, W. H. Merigan, J. G. Flannery, D.V. Schaffer, In vivo–directed evolution of a new adeno-associated virus for therapeutic outer retinal gene delivery from the vitreous. Sci. Transl. Med. 5, 189ra76 (2013).

6) E. MacLaren, R. A. Pearson, A. MacNeil, R. H. Douglas, T. E. Salt, M. Akimoto, A. Swaroop, J. C. Sowden, R. R. Ali, Retinal repair by transplantation of photoreceptor precursors. Nature 444, 203–207 (2006).

7) M. S. Singh, P. Charbel Issa, R. Butler, C. Martin, D. M. Lipinski, S. Sekaran, A. R. Barnard,

R. E. MacLaren, Reversal of end-stage retinal degeneration and restoration of visual function by photoreceptor transplantation. Proc. Natl. Acad. Sci. U.S.A.110, 1101–1106 (2013)

8) DeAngelis MM, Silveira AC, Carr EA, Kim IK. Genetics of Age-Related Macular Degeneration: Current Concepts, Future Directions. *Seminars in ophthalmology*. 2011;26(3):77-93. doi:10.3109/08820538.2011.577129.

9) Thumann G. Prospectives for Gene Therapy of Retinal Degenerations. *Current Genomics*. 2012;13(5):350-362. doi:10.2174/138920212801619214.

10) Schwartz, S.D., Tan, G., Hosseini, H., & Nagiel, A. (2016). Subretinal Transplantation of Embryonic Stem Cell–Derived Retinal Pigment Epithelium for the Treatment of Macular Degeneration: An Assessment at 4 YearshESC-RPE Transplantation. *Invest. Ophthalmol. Vis. Sci., 57* (5), ORSFc1-ORSFc9.

11) W. K. Song, K.-M. Park, H.-J. Kim, J. H. Lee, J. Choi, S. Y. Chong, S. H. Shim, L. V. Del Priore, R. Lanza, Treatment of macular degeneration using embryonic stem cell-derived retinal pigment epithelium: Preliminary results in Asian patients. Stem Cell Reports 4, 860–872 (2015).

12) Divya Sinha, Jenny Phillips, M. Joseph Phillips, David M. Gamm; Mimicking Retinal Development and Disease With Human Pluripotent Stem Cells. *Invest. Ophthalmol. Vis. Sci.* 2016;57(5)

13) Bramall A.N., Wright A.F., Jacobson S.G., McInnes R.R. "The genomic, biochemical, and cellular responses of the retina in inherited photoreceptor degenerations and prospects for the treatment of these disorders."Annu. Rev. Neurosci. 2010;33:441–472.

14) Reynolds, Joseph, and Deepak A. Lamba. "Human Embryonic Stem Cell Applications for Retinal Degenerations." *Experimental Eye Research* 123 (2014): 151-60.

15) Reh, T.A. (2016). Photoreceptor Transplantation in Late Stage Retinal Degeneration. *Invest. Ophthalmol. Vis. Sci., 57* (5).

16) Barber, A.C., Hippert, C., Duran, Y., West, E.L., Bainbridge, J.W.B., Warre-Cornish, K., Luhmann, U.F.O., Lakowski, J., Sowden, J.C., Ali, R.R., Pearson, R.A., 2013. Repair of the degenerate retina by photoreceptor transplantation. Proc Natl Acad Sci USA 110, 354-359

17)McUsic AC, Lamba DA, Reh TA. Guiding the morphogenesis of dissociated newborn mouse retinal cells and hES cell-derived retinal cells by soft lithography-patterned microchannel PLGA scaffolds. *Biomaterials*. 2012;**33**:1396-1405.

18) Redenti S, Tao S, Yang J, et al. Retinal tissue engineering using mouse retinal progenitor cells and a novel biodegradable, thin-film poly(e-caprolactone) nanowire scaffold. *J Ocul Biol Dis Infor*. 2008;**1**:19- 29.

19) Osakada F, Ikeda H, Mandai M, et al. Toward the generation of rod and cone photoreceptors from mouse, monkey and human embryonic stem cells. *Nat Biotechnol*. 2008; **26**:215-224.

20) Herberts CA, Kwa MS, Hermsen HP. Risk factors in the development of stem cell therapy. *Journal of Translational Medicine*. 2011;9:29..

21) Robert E. MacLaren, Jean Bennett, Steven D. Schwartz, Gene Therapy and Stem Cell Transplantation in Retinal Disease: The New Frontier, Ophthalmology, Volume 123, Issue 10, Supplement, October 2016, Pages S98-S106.

22) Li, Y.; Tsai, Y.T.; Hsu, C.W.; Erol, D.; Yang, J.; Wu, W.H.; Davis, R.J.; Egli, D.; Tsang, S.H. Long-term safety and efficacy of human-induced pluripotent stem cell (iPS) grafts in a preclinical model of retinitis pigmentosa. Mol. Med. 2012, 18, 1312–1319.

23) Hatori M, Panda S. The emerging roles of melanopsin in behavioral adaptation to light. *Trends in molecular medicine*. 2010;16(10):435-446.

24) Gargini C, Terzibasi E, Mazzoni F, Strettoi E. *I*Retinal Organization in the retinal degeneration 10 (rd10) Mutant Mouse: a Morphological and ERG Study. *The Journal of comparative neurology*. 2007;500(2):222-238.

25)Danciger M, Blaney J, Gao YQ, Zhao DY, Heckenlively JR, Jacobson SG, Farber DB.

"Mutations in the PDE6B gene in autosomal recessive retinitis pigmentosa". *Genomics.* 1995;30:1–7.

26) Eiraku, M. *et al*. Self-organizing optic-cup morphogenesis in three-dimensional culture. Nature 472, 51–56 (2011)

27) Kundu, J., Michaelson, A., Talbot, K., Baranov, P., Young, M.J., & Carrier, R.L. (2016). Decellularized retinal matrix: Natural platforms for human retinal progenitor cell culture. *Acta Biomater., 31*, 61-70.

28) Lai, J.-Y. (2010). Biocompatibility of chemically cross-linked gelatin hydrogels for ophthalmic use. *J. Mater. Sci. Mater. Med. , 21* (6), 1899-1911

29) Santos-Ferreira, T., Llonch, S., Borsch, O., Postel, K., Haas, J., & Ader, M. (2016). Retinal transplantation of photoreceptors results in donor–host cytoplasmic exchange. *Nat. Commun., 7,* 13028.

30) Pearson RA, Barber AC, Rizzi M, et al. Restoration of vision after transplantation of photoreceptors. *Nature*. 2012;485(7396):99-103. doi:10.1038/nature10997.

Supplemental material:

**Table 1- qRT-PCR primers**

| Genes | Forward Sequence 5'-3' | Reverse Sequence 3'-5' | Size (bp) |
|---|---|---|---|
| BRN3 | CTC ACA CTG TCC CAC AAT AAT A | CCG GCG GAA TAT TTC ATT CT | 311 |
| CHX10 | ATT CAA CGA AGC CCA CTA CCC AGA | ATC CTT GGC TGA CTT GAG GAT GGA | 229 |
| CRX | TAT TCT GTC AAC GCC TTG GCC CTA | TGC ATT TAG CCC TCC GGT TCT TGA | 253 |
| LHX2 | CAA GAT CTC GGA CCG CTA CT | CCG TGG TCA GCA TCT TGT TA | 284 |
| NANOG | CAA AGG CAA ACA ACC CAC TT | TCT GCT GGA GGC TGA GGT AT | 158 |
| NEUROD1 | TAC TGC TGC AAA GTG CAA ATA C | AAG TGC TAA GGC AAC ACA ATA AC | 539 |
| OCT4 | CGA GCA ATT TGC CAA GCT CCT GAA | TTC GGG CAC TGC AGG AAC AAA TTC | 324 |
| OTX2 | CAA CAG CAG AAT GGA GGT CA | CTG GGT GGA AAG AGA GAA GC TG | 429 |
| PAX6 | CGG AGT GAA TCA GCT CGG TG | CCG CTT ATA CTG GGC TAT TTT GC | 300 |
| RAX | GAA TCT CGA AAT CTC AGC CC | CTT CAC TAA TTT GCT CAG GAC | 279 |
| SIX3 | CGA GCA GAA GAC GCA TTG CTT CAA | CGG CCT TGG CTA TCA TAC ATC ACA | 394 |
| SIX6 | ATT TGG GAC GGC GAA CAG AAG ACA | ATC CTG GAT GGG CAA CTC AGA TGT | 385 |
| GAPDH | TCACCAGGGCTGCTTTTAAC | GACAAGCTTCCCGTTCTCAG | 153 |

**Table 2- Antibody used for immunofluorescence**

| Antibody | Type | Source | Dilution |
|---|---|---|---|
| Sox2 | Rabbit polyclonal | Abcam | IF 1:100 |
| OTX2 | Rabbit polyclonal | Novus Biologicals | IF 1:100 |
| PAX6 | Rabbit polyclonal | Abgent | IF 1:200 |
| LHX2 | Goat polyclonal | Santa Cruz Biotechnology | IF1:200 |
| CHX10/VSX2 | Sheep monoclonal | EMD Millipore | IF, 1:200 |
| RAX | Mouse monoclonal | Abnova | IF, 1:500 |
| Rhodopsin | Rabbit monoclonal | Cell Signaling | IF, 1:300 |
| CRX | Rabbit polyclonal | Novus Biologicals | IF, 1:200 |
| β-Tubulin-III | Rabbit polyclonal | Abcam | IF, 1:1500 |
| Ki67 | Rabbit polyclonal | Thermo Scientifics | IF,1:500 |
| CRX | Rabbit monoclonal | Novus Biologicals | IF,1:200 |
| Recoverin | Rabbit polyclonal | EMD Millipore | IF, 1:300 |
| TRA-1-85 | Mouse monoclonal | EMD Millipore | IF, 1:200 |
| IL-6 | Mouse monoclonal | Abcam | IF, 1:200 |
| IBA-1 | Goat monoclonal | Abcam | IF, 1:200 |